Mathematical Biosciences and Engineering

http://www.aimspress.com/journal/mbe

MBE, 19(12): 13028–13049.
DOI: 10.3934/mbe.2022608
Received: 17 June 2022
Revised: 22 August 2022
Accepted: 29 August 2022
Published: 05 September 2022

Research article

Modelling and stability analysis of ASFV with swill and the virus in the environment

Haitao Song[1,2,*], **Lirong Guo**[1,2,3], **Zhen Jin**[1,2] **and Shengqiang Liu**[4,*]

[1] Complex Systems Research Center, Shanxi University, Taiyuan 030006, China
[2] Shanxi Key Laboratory of Mathematical Techniques and Big Data Analysis, on disease Control and Prevention, Shanxi University, Taiyuan 030006, China
[3] School of Mathematical Sciences, Shanxi University, Taiyuan 030006, China
[4] School of Mathematical Sciences, Tiangong University, Tianjin 300387, China

* **Correspondence:** Email: htsong@sxu.edu.cn (H. Song), sqliu@tiangong.edu.cn (S. Liu).

Abstract: African swine fever (ASF) is an acute, hemorrhagic and severe infectious disease caused by the African swine fever virus (ASFV), and leads to a serious threat to the pig industry in China. Yet the impact of the virus in the environment and contaminated swill on the ASFV transmission is unclear in China. Then we build the ASFV transmission model with the virus in the environment and swill. We compute the basic reproduction number, and prove that the disease-free equilibrium is globally asymptotically stable when $R_0 < 1$ and the unique endemic equilibrium is globally asymptotically stable when $R_0 > 1$. Using the public information, parameter values are evaluated. PRCCs and eFAST sensitivity analysis reveal that the release rate of ASFV from asymptomatic and symptomatic infectious pigs and the proportion of pig products from infectious pigs to swill have a significant impact on the ASFV transmission. Our findings suggest that the virus in the environment and contaminated swill contribute to the ASFV transmission. Our results may help animal health to prevent and control the ASFV transmission.

Keywords: African swine fever; mathematical model; swill; sensitivity analysis; global stability

1. Introduction

African swine fever virus (ASFV) is an ancient virus and was first discovered in 1921 in Kenya. African swine fever (ASF) is caused by ASFV which is a large double-stranded DNA virus, and ASF is a highly contagious hemorrhagic disease of pigs [1, 2]. Pigs of all breeds and ages can be infected [3], and the outbreaks of ASF lead to a mass of death of pigs [4, 5]. The clinical manifestation includes high fever, bleeding, and other symptoms [6]. In general, the incubation period ranges from 4 to

19 days [2]. For highly pathogenic ASFV strains, the fatality rate could reach 100% [7]. Since the outbreak in East Africa in the 1900s, the spread of ASF ranges from Africa and Europe to South America and Caribbean [8]. Ever since the first outbreak was reported in Shenyang in August 2018, ASF has quickly spread in China and led to millions of pigs culled [9]. In the absence of a vaccine, ASF poses a serious threat to the domestic and foreign trade of pigs and pork products [10, 11].

ASF could be transmitted by direct transmission and indirect transmission. The direct transmission includes the direct contact between susceptible pigs and infected pigs (effective transmission distance within 1 km), and feeding contaminated pig products [12–14]. The indirect transmission occurs by the virus in the environment and ticks [4]. The important routes of transmission of ASF may be feeding noxious swill and exposure to the virus from infected pigs, and other possible routes for the spread of ASFV in China may be the widespread use of contaminated swill and pig products [15]. Thus, the virus in the environment and contaminated swill play an important role in the ASFV transmission.

Mathematical modeling is an important method to explore the spread of diseases such as ASF, and prevent and control the disease spreading using public information [16–24]. Guinat et al. [25] used a stochastic SEIR model to estimate the basic reproduction number in Georgia. Barongo et al. [26] developed a stochastic dynamical model to evaluate the impact of control strategies at different times on disease-related mortality. O'Neill et al. [27] developed a wild boar ASF model to explore the pivotal transmission and infection maintenance processes. Based on the effectiveness of control measures, Li et al. [28] proposed a generalized SEIR model and estimated the important epidemiological parameter values. Although some research focuses on the dynamics of ASFV transmission, little research contributes to the impact of contaminated swill and virus in the environment on the ASFV transmission so far.

In this paper, to examine the impact of contaminated swill and virus in the environment on the ASFV transmission, we propose an ASFV transmission model with swill and virus in the environment. The basic reproduction number is computed using the next-generation matrix. We prove the global stability of the disease-free equilibrium and endemic equilibrium by constructing the Lyapunov function. Based on the public information, parameter values are estimated, and sensitivity analysis will be performed by PRCC and eFAST. Numerical simulations are implemented to validate the theoretical results and assess the impact of contaminated swill and virus in the environment on the ASFV transmission.

This paper is organized as follows. In Section 2, we formulate an ASF transmission dynamics model, and the nonnegativeness and boundedness of solutions are proved. In Section 3, the basic reproduction number is calculated, and the global dynamics are proved. In Section 4, parameter values are estimated using the reported cases in Aijuan, and sensitivity analysis and numerical simulations are implemented. Section 5 gives the conclusion and discussion.

2. Model formulation

Based on the mechanism of ASFV transmission [29, 30], the population of the pig is divided into susceptible pigs (S), asymptomatic infectious pigs (I_1) and symptomatic infectious pigs (I_2). Also, ASFV is transmitted by feeding contaminated swill and contact with the virus in the environment. Then we assume that V denotes the virus load in the environment and W denotes the amount of contaminated swills. Given the mechanism of ASFV transmission and previous work [27, 28], we build the ASFV

transmission model

$$\begin{cases} \dfrac{dS(t)}{dt} = b - d_1 S(t) - \beta_1 S(t) I_1(t) - \beta_2 S(t) I_2(t) - \beta_3 S(t) V(t) - \beta_4 S(t) W(t), \\ \dfrac{dI_1(t)}{dt} = \beta_1 S(t) I_1(t) + \beta_2 S(t) I_2(t) + \beta_3 S(t) V(t) + \beta_4 S(t) W(t) - (\alpha + d_1) I_1(t), \\ \dfrac{dI_2(t)}{dt} = \alpha I_1(t) - d_2 I_2(t), \\ \dfrac{dV(t)}{dt} = \delta_1 I_1(t) + \delta_2 I_2(t) - c_1 V(t), \\ \dfrac{dW(t)}{dt} = p_1 I_1(t) + p_2 I_2(t) - c_2 W(t), \end{cases} \tag{2.1}$$

with nonnegative initial values

$$S(0) > 0, I_1(0) \geq 0, I_2(0) \geq 0, V(0) \geq 0 \text{ and } W(0) \geq 0, \tag{2.2}$$

where $p_1 = pd_1, p_2 = pd_2$. The detailed descriptions of state variables and related parameters in model (2.1) are shown in Table 1. The flow chart in Figure 1 depicts the transmission of ASFV.

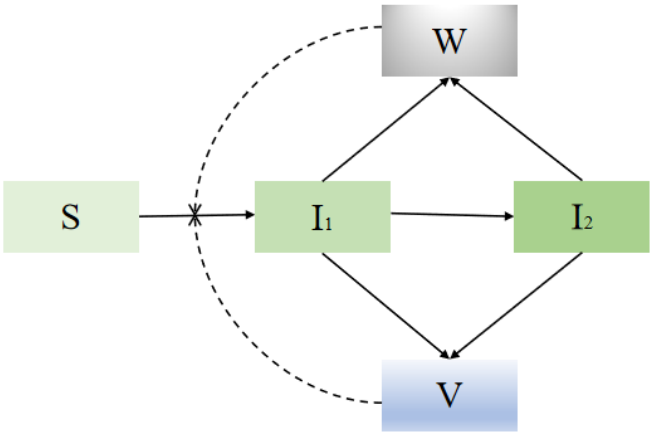

Figure 1. The flow chart of ASFV transmission.

Theorem 2.1. *The solutions of the model (2.1) with nonnegative initial values (2.2) are nonnegative and ultimately bounded.*

Proof. Form model (2.1) with nonnegative initial values (2.2), we can get

$$S(t) = e^{-\int_0^t (d_1+\beta_1 I_1(s)+\beta_2 I_2(s)+\beta_3 V(s)+\beta_4 W(s))ds}(S(0) + \int_0^t be^{\int_0^s K_1 d\gamma} ds) > 0$$

where

$$K_1 = (d_1 + \beta_1 I_1(\gamma) + \beta_2 I_2(\gamma) + \beta_3 V(\gamma) + \beta_4 W(\gamma)),$$

Table 1. Description of state variable and related parameters in model (2.1).

Parameter	Description	Units
b	The recruitment rate of pigs	head/day
β_1	The transmission rate from asymptomatic infectious pigs to susceptible pigs	1/(head.day)
β_2	The transmission rate from symptomatic infectious pigs to susceptible pigs	1/(head.day)
β_3	The transmission rate from virus in environment to susceptible pigs	1/(TCID50.day)
β_4	The transmission rate from swill to susceptible pigs	1/(kg.day)
d_1	The removal rate of asymptomatic infectious pigs including slaughtering and death pigs including slaughtering and death	1/day
d_2	The removal rate of symptomatic infectious pigs including slaughtering and death	1/day
c_1	The clearance rate of virus in environment	1/day
c_2	The clearance rate of swill	1/day
δ_1	The release rate of ASFV from asymptomatic infectious pigs	TCID50/(head.day)
δ_2	The release rate of ASFV from symptomatic infectious pigs	TCID50/(head.day)
p	The proportion of pig products from infectious pigs to swill	none
α	The transfer rate from asymptomatic infectious pigs to symptomatic infectious pigs	1/day
State variables	**Description**	**Units**
S	The susceptible pigs	head
I_1	The asymptomatic infectious pigs	head
I_2	The symptomatic infectious pigs	head
V	The virus load in the environment	TCID50
W	The amount of contaminated swills	kg

$$I_1(t) = e^{-\int_0^t (\alpha+d_1)ds}(I_1(0) + \int_0^t K_2 e^{\int_s^t (\alpha+d_1)d\epsilon} ds)$$

where

$$K_2 = (\beta_1 S(s)I_1(s) + \beta_2 S(s)I_2(s) + \beta_3 S(s)V(s) + \beta_4 S(s)W(s)),$$

and

$$I_2(t) = e^{-\int_0^t d_2 ds}(I_2(0) + \int_0^t (\alpha I_1(s))e^{\int_s^t d_2 d\epsilon} ds),$$

$$V(t) = e^{-\int_0^t c_1 ds}(V(0) + \int_0^t (\delta_1 I_1(s) + \delta_2 I_2(s))e^{\int_s^t c_1 d\epsilon} ds),$$

$$W(t) = e^{-\int_0^t c_2 ds}(W(0) + \int_0^t (pd_1 I_1(s) + pd_2 I_2(s))e^{\int_s^t c_2 d\epsilon} ds)$$

with $S(t) \geq 0, I_1(t) \geq 0, I_2(t) \geq 0, V(t) \geq 0$ and $W(t) \geq 0$. Therefore, the nonnegativity of solutions is proved.

Now, we prove the ultimate boundedness of solutions. From the model (2.1),

$$\frac{d(S(t) + I_1(t) + I_2(t))}{dt} = b - d_1 S(t) - d_1 I_1(t) - d_2 I_2(t) \leq b - d(S(t) + I_1(t) + I_2(t)),$$

where $d = \min\{d_1, d_2\}$. According to the comparison theorem [31], we have

$$\limsup_{t\to\infty}(S(t) + I_1(t) + I_2(t)) \leq \frac{b}{d}, \ \limsup_{t\to\infty} V(t) \leq \frac{b(\delta_1 + \delta_2)}{c_1 d}, \ \limsup_{t\to\infty} W(t) \leq \frac{b(pd_1 + pd_2)}{c_2 d}.$$

Therefore, the nonnegativity and boundedness of solutions of model (2.1) are proved. □

The feasible region

$$\Omega = \{(S, I_1, I_2, V, W) \in R_+^5 : S + I_1 + I_2 \leq \frac{b}{d}, V \leq \frac{b(\delta_1 + \delta_2)}{c_1 d}, W \leq \frac{b(pd_1 + pd_2)}{c_2 d}\},$$

is the positive invariant set of model (2.1).

3. Threshold dynamics

3.1. The basic reproduction number and equilibria

Obviously, system (2.1) always has a disease-free equilibrium $E_0 = (S_0, 0, 0, 0, 0)$, where $S_0 = b/d_1$. Using the theory in [32], we could compute the basic reproduction number. Let $X = (I_1, I_2, V, W)$, then model (2.1) can be expressed as

$$\frac{dX(t)}{dt} = \mathscr{F} - \mathscr{V},$$

where

$$\mathscr{F} = \begin{pmatrix} \beta_1 S(t) I_1(t) + \beta_2 S(t) I_2(t) + \beta_3 S(t) V(t) + \beta_4 S(t) W(t) \\ 0 \\ 0 \\ 0 \end{pmatrix},$$

$$\mathscr{V} = \begin{pmatrix} \alpha I_1(t) + d_1 I_1(t) \\ -\alpha I_1(t) + d_2 I_2(t) \\ -\delta_1 I_1(t) - \delta_2 I_2(t) + c_1 V(t) \\ -pd_1 I_1(t) - pd_2 I_2(t) + c_2 W(t) \end{pmatrix}.$$

The Jacobian matrices of $\mathscr{F}$ and $\mathscr{V}$ at E_0 gives

$$F = \begin{pmatrix} \beta_1 S_0 & \beta_2 S_0 & \beta_3 S_0 & \beta_4 S_0 \\ 0 & 0 & 0 & 0 \\ 0 & 0 & 0 & 0 \\ 0 & 0 & 0 & 0 \end{pmatrix}, V = \begin{pmatrix} \alpha + d_1 & 0 & 0 & 0 \\ -\alpha & d_2 & 0 & 0 \\ -\delta_1 & -\delta_2 & c_1 & 0 \\ -pd_1 & -pd_2 & 0 & c_2 \end{pmatrix}.$$

Using the spectral radius of the matrix FV^{-1}, we have the basic reproduction number

$$R_0 = \frac{\beta_1 S_0}{(\alpha + d_1)} + \frac{\alpha\beta_2 S_0}{(\alpha + d_1)d_2} + \frac{(\delta_1 d_2 + \delta_2\alpha)\beta_3 S_0}{c_1(\alpha + d_1)d_2} + \frac{p(d_2\alpha + d_1 d_2)\beta_4 S_0}{c_2 d_2(\alpha + d_1)}.$$

When $R_0 > 1$, the unique endemic equilibrium of model (2.1) is $E_1(S^*, I_1^*, I_2^*, V^*, W^*)$, where

$$S^* = \frac{S_0}{R_0},\ \ I_1^* = \frac{b}{\alpha + d_1}(1 - \frac{1}{R_0}),\ \ I_2^* = \frac{\alpha I_1^*}{d_2},\ \ V^* = \frac{\delta_1 I_1^* + \delta_2 I_2^*}{c_1},\ \ W^* = \frac{pd_1 I_1^* + pd_2 I_2^*}{c_2}.$$

3.2. Local stability

Theorem 3.1. *When $R_0 < 1$, the disease-free equilibrium $E_0 = (S_0, 0, 0, 0, 0)$ of model (2.1) is locally asymptotically stable in Ω.*

Proof. The Jacobian matrix J_1 at E_0 gives

$$J_1 = \begin{pmatrix} -d_1 & -\beta_1 S_0 & -\beta_2 S_0 & -\beta_3 S_0 & -\beta_4 S_0 \\ 0 & \beta_1 S_0 - \alpha - d_1 & \beta_2 S_0 & \beta_3 S_0 & \beta_4 S_0 \\ 0 & \alpha & -d_2 & 0 & 0 \\ 0 & \delta_1 & \delta_2 & -c_1 & 0 \\ 0 & pd_1 & pd_2 & 0 & -c_2 \end{pmatrix}.$$

Obviously, the characteristic equation of J_1 always has a negative real root $\lambda_1 = -d_1$, and the other roots are determined by the following equation

$$\begin{aligned}(\lambda + \alpha + d_1)(\lambda + d_2)(\lambda + c_1)(\lambda + c_2) =& \beta_1 S_0(\lambda + c_2)(\lambda + d_2)(\lambda + c_1) + \alpha\beta_2 S_0(\lambda + c_1)(\lambda + c_2) \\ &+ \beta_3 S_0\alpha\delta_2(\lambda + c_2) + \beta_3 S_0\delta_1(\lambda + d_2)(\lambda + c_2) \\ &+ \beta_4 S_0((\lambda + d_2)(\lambda + c_1)pd_1 + (\lambda + c_1)pd_2\alpha).\end{aligned}$$

Assume that $Re(\lambda) \geq 0$. Then we can divide by $(\lambda + \alpha + d_1)(\lambda + d_2)(\lambda + c_1)(\lambda + c_2)$ and take absolute values on both sides of the equation, and we have

$$\begin{aligned}1 =& \Big|\frac{\beta_1 S_0}{(\lambda + \alpha + d_1)} + \frac{\alpha\beta_2 S_0}{(\lambda + \alpha + d_1)(\lambda + d_2)} + \frac{\delta_2\alpha\beta_3 S_0}{(\lambda + \alpha + d_1)(\lambda + d_2)(\lambda + c_1)} \\ &+ \frac{\beta_3\delta_1 S_0}{(\lambda + \alpha + d_1)(\lambda + c_1)} + \frac{\beta_4 S_0 pd_1}{(\lambda + \alpha + d_1)(\lambda + c_2)} + \frac{\beta_4 S_0 pd_2\alpha}{(\lambda + \alpha + d_1)(\lambda + c_2)(\lambda + d_2)}\Big|.\end{aligned}$$

If $\lambda = x + yi$, where i is the imaginary unit, then

$$|(\lambda + \alpha + d_1)| \geq (x + \alpha + d_1) \geq (\alpha + d_1),$$

$$|(\lambda + \alpha + d_1)(\lambda + d_2)| \geq (x + \alpha + d_1)(x + d_2) \geq (\alpha + d_1)d_2,$$

$$|(\lambda + \alpha + d_1)(\lambda + d_2)(\lambda + c_1)| \geq (x + \alpha + d_1)(x + d_2)(x + c_1) \geq (\alpha + d_1)d_2c_1,$$

$$|(\lambda + \alpha + d_1)(\lambda + c_2)(\lambda + d_2)| \geq (x + \alpha + d_1)(x + c_2)(x + d_2) \geq (\alpha + d_1)d_2c_2,$$

Hence,

$$1 \leq \Big|\frac{\beta_1 S_0}{(\lambda + \alpha + d_1)}\Big| + \Big|\frac{\alpha\beta_2 S_0}{(\lambda + \alpha + d_1)(\lambda + d_2)}\Big|$$

$$
\begin{aligned}
&+\left|\frac{\delta_2\alpha\beta_3 S_0}{(\lambda+\alpha+d_1)(\lambda+d_2)(\lambda+c_1)}\right|+\left|\frac{\beta_3 S_0\delta_1}{(\lambda+\alpha+d_1)(\lambda+c_1)}\right|\\
&+\left|\frac{\beta_4 S_0 pd_1}{(\lambda+\alpha+d_1)(\lambda+c_2)}\right|+\left|\frac{\beta_4 S_0 pd_2\alpha}{(\lambda+\alpha+d_1)(\lambda+c_2)(\lambda+d_2)}\right|\\
&\le \frac{\beta_1 S_0}{(\alpha+d_1)}+\frac{\alpha\beta_2 S_0}{(\alpha+d_1)d_2}+\frac{\delta_2\alpha\beta_3 S_0}{(\alpha+d_1)d_2c_1}+\frac{\beta_3 S_0\delta_1}{(\alpha+d_1)c_1}\\
&+\frac{\beta_4 S_0 pd_1}{(\alpha+d_1)c_2}+\frac{\beta_4 S_0 pd_2\alpha}{(\alpha+d_1)c_2d_2}=R_0,
\end{aligned}
$$

which contradicts with $R_0 < 1$. All roots of characteristic equation have negative parts when $R_0 < 1$. Thus, the disease-free equilibrium of model (2.1) is locally asymptotically stable in Ω. □

Theorem 3.2. *When $R_0 > 1$, the unique endemic equilibrium $E_1(S^*, I_1^*, I_2^*, V^*, W^*)$ of model (2.1) is locally asymptotically stable in Ω.*

Proof. The Jacobian matrix J_2 at E_1 gives

$$
J_2=\begin{pmatrix}
-d_1-\beta_1 I_1^*-\beta_2 I_2^*-\beta_3 V^*-\beta_4 W^* & -\beta_1 S^* & -\beta_2 S^* & -\beta_3 S^* & -\beta_4 S^*\\
\beta_1 I_1^*+\beta_2 I_2^*+\beta_3 V^*+\beta_4 W^* & \beta_1 S^*-\alpha-d_1 & \beta_2 S^* & \beta_3 S^* & \beta_4 S^*\\
0 & \alpha & -d_2 & 0 & 0\\
0 & \delta_1 & \delta_2 & -c_1 & 0\\
0 & pd_1 & pd_2 & 0 & -c_2
\end{pmatrix}.
$$

The characteristic equation of J_2 leads to

$$
\begin{aligned}
&(\beta_1 I_1^*+\beta_2 I_2^*+\beta_3 V^*+\beta_4 W^*)[(\lambda+\alpha+d_1)(\lambda+d_2)(\lambda+c_1)(\lambda+c_2)]+A\\
&=pd_1(\lambda+d_1)\beta_4 S^*(\lambda+d_2)(\lambda+c_1)+pd_2(\lambda+d_1)(\lambda+c_1)\beta_4 S^*\alpha\\
&+(\lambda+d_1)(\lambda+d_2)(\lambda+c_1)(\lambda+c_2)\beta_1 S^*+(\lambda+d_1)(\lambda+c_2)\beta_3 S^*\alpha\delta_2\\
&+(\lambda+d_1)(\lambda+c_2)(\lambda+d_2)\beta_3 S^*\delta_1+(\lambda+d_1)(\lambda+c_2)(\lambda+c_1)\beta_2 S^*\alpha,
\end{aligned}
$$

where

$$
A=(\lambda+d_1)(\lambda+\alpha+d_1)(\lambda+d_2)(\lambda+c_1)(\lambda+c_2).
$$

Using the similar discussion in Theorem 3.1, we assume that $Re(\lambda)\ge 0$. Then we can divide the two sides of the above equation by A and take the absolute value of both sides of this equation, and we have

$$
1+\frac{(\beta_1 I_1^*+\beta_2 I_2^*+\beta_3 V^*+\beta_4 W^*)}{(\lambda+d_1)}>1.
$$

The right side of equation gives

$$
\begin{aligned}
&\left|\frac{\beta_1 S^*}{(\lambda+\alpha+d_1)}+\frac{\beta_2 S^*\alpha}{(\lambda+\alpha+d_1)(\lambda+d_2)}+\frac{\beta_3 S^*\alpha\delta_2}{(\lambda+\alpha+d_1)(\lambda+c_1)(\lambda+d_2)}\right.\\
&\left.+\frac{\beta_3 S^*\delta_1}{(\lambda+\alpha+d_1)(\lambda+c_1)}+\frac{pd_1\beta_4 S^*}{(\lambda+c_2)(\lambda+\alpha+d_1)}+\frac{pd_2\beta_4 S^*\alpha}{(\lambda+\alpha+d_1)(\lambda+c_2)(\lambda+d_2)}\right|\\
&\le\frac{\beta_1 S^*}{(\alpha+d_1)}+\frac{\beta_2 S^*\alpha}{(\alpha+d_1)d_2}+\frac{\beta_3 S^*\alpha\delta_2}{(\alpha+d_1)(\lambda+c_1)d_2}+\frac{\beta_3 S^*\delta_1}{(\alpha+d_1)c_1}+\frac{pd_1\beta_4 S^*}{c_2(\alpha+d_1)}
\end{aligned}
$$

$$+\frac{pd_2\beta_4 S^*\alpha}{(\alpha+d_1)c_2)d_2} \le \frac{1}{R_0}R_0 = 1,$$

which leads to a contradiction. All roots of characteristic equation have negative parts when $R_0 > 1$. Thus, the unique endemic equilibrium of model (2.1) is locally asymptotically stable in Ω. □

3.3. Global dynamics

In this section, we prove that the disease-free equilibrium and endemic equilibrium of model (2.1) are globally asymptotically stable by constructing Lyapunov function. Let

$$F(x) = x - 1 - \ln x, x \in (0, \infty).$$

Note that $F(x) \ge 0$ when $x > 0$, and $F_{\min}(x) = F(1) = 0$.

Theorem 3.3. *When $R_0 < 1$, the disease-free equilibrium $E_0 = (S_0, 0, 0, 0, 0)$ of model (2.1) is globally asymptotically stable in Ω.*

Proof. Define the Lyapunov function

$$L_0(t) = S_0 F\Big(\frac{S(t)}{S_0}\Big) + I_1(t) + \frac{c_1c_2\beta_2 b + \delta_2 c_2\beta_3 b + c_1\beta_4 bpd_2}{c_1c_2d_1d_2}I_2(t) + \frac{\beta_3 b}{c_1d_1}V(t) + \frac{\beta_4 b}{c_2d_1}W(t).$$

The time derivative of L_0 along the solution of model (2.1) gives

$$\begin{aligned}
\frac{dL_0(t)}{dt}\Big|_{(2.1)} &= \Big(1 - \frac{S_0}{S(t)}\Big)(b - d_1S(t) - \beta_1S(t)I_1(t) - \beta_2S(t)I_2(t) - \beta_3S(t)V(t) - \beta_4S(t)W(t)) \\
&\quad + (\beta_1S(t)I_1(t) + \beta_2S(t)I_2(t) + \beta_3S(t)V(t) + \beta_4S(t)W(t) - \alpha I_1(t) - d_1I_1(t)) \\
&\quad + \frac{c_1c_2\beta_2 b + \delta_2c_2\beta_3 b + c_1\beta_4 bpd_2}{c_1c_2d_1d_2}(\alpha I_1(t) - d_2I_2(t)) \\
&\quad + \frac{\beta_3 b}{c_1d_1}(\delta_1I_1(t) + \delta_2I_2(t) - c_1V(t)) + \frac{\beta_4 b}{c_2d_1}(pd_1I_1(t) + pd_2I_2(t) - c_2W(t)) \\
&= -\frac{d_1(S(t) - S_0)^2}{S(t)} + \Big(\frac{\beta_1 bI_1(t)}{d_1} + \frac{\beta_2 bI_2(t)}{d_1} + \frac{\beta_3 bV(t)}{d_1} + \frac{\beta_4 bW(t)}{d_1}\Big) \\
&\quad - \alpha I_1(t) - d_1I_1(t) + \frac{c_1c_2\beta_2 b + \delta_2c_2\beta_3 b + c_1\beta_4 bpd_2}{c_1c_2d_1d_2}(\alpha I_1(t) - d_2I_2(t)) \\
&\quad + \frac{\beta_3 b}{c_1d_1}(\delta_1I_1(t) + \delta_2I_2(t) - c_1V(t)) + \frac{\beta_4 b}{c_2d_1}(pd_1I_1(t) + pd_2I_2(t) - c_2W(t)) \\
&= -\frac{d_1(S(t) - S_0)^2}{S(t)} + \Big(\frac{\beta_3 b}{d_1} - \frac{\beta_3 b}{d_1}\Big)V(t) + \Big(\frac{\beta_4 b}{d_1} - \frac{\beta_4 b}{d_1}\Big)W(t) \\
&\quad + \Big(\frac{\beta_1 b}{d_1} - (\alpha + d_1) + \frac{\alpha c_1c_2\beta_2 b + \alpha\delta_2c_2\beta_3 b + \alpha c_1\beta_4 bpd_2}{c_1c_2d_1d_2} + \frac{\beta_3 b\delta_1}{c_1d_1} + \frac{\beta_4 bpd_1}{c_2d_1}\Big)I_1(t) \\
&\quad + \Big(\frac{\beta_2 b}{d_1} - \frac{c_1c_2\beta_2 b + \delta_2c_2\beta_3 b + c_1\beta_4 bpd_2}{c_1c_2d_1} + \frac{\beta_3 b\delta_2}{c_1d_1} + \frac{\beta_4 bpd_2}{c_2d_1}\Big)I_2(t) \\
&\le -\frac{d_1(S(t) - S_0)^2}{S(t)} + (R_0 - 1)I_1(t).
\end{aligned}$$

Note that $L_0'(t) < 0$ when $R_0 < 1$. In addition, $L_0'(t) = 0$ if and only if $S = S_0, I_1 = 0, I_2 = 0, V = 0, W = 0$. The single point set E_0 is the largest invariant set of model (2.1) on set $\{(S(t), I_1(t), I_2(t), V(t), W(t)) \in \Omega \mid L_0'(t) = 0\}$. Using LaSalle's Invariance Principle [33] and the local stability of E_0, then the disease-free equilibrium E_0 is globally asymptotically stable in Ω when $R_0 < 1$. □

Theorem 3.4. *When $R_0 > 1$, the unique endemic equilibrium $E_1(S^*, I_1^*, I_2^*, V^*, W^*)$ of model (2.1) is globally asymptotically stable in Ω.*

Proof. Define the Lyapunov function

$$\begin{aligned} L_1(t) =& S^* F\Big(\frac{S(t)}{S^*}\Big) + I_1^* F\Big(\frac{I_1(t)}{I_1^*}\Big) + \Big(\frac{c_1c_2\beta_2S^* + c_2\beta_3S^*\delta_2 + c_1\beta_4S^*pd_2}{c_1c_2d_2}\Big)I_2^* F\Big(\frac{I_2(t)}{I_2^*}\Big) \\ &+ \frac{\beta_3S^*}{c_1}V^* F\Big(\frac{V(t)}{V^*}\Big) + \frac{\beta_4S^*}{c_2}W^* F\Big(\frac{W(t)}{W^*}\Big). \end{aligned}$$

Calculating the derivative of $L_1(t)$ along the solution of model (2.1) gives

$$\begin{aligned} \frac{dL_1(t)}{dt}\Big|_{(2.1)} =& \Big(1 - \frac{S^*}{S(t)}\Big)(b - d_1S(t) - \beta_1S(t)I_1(t) - \beta_2S(t)I_2(t) - \beta_3S(t)V(t) - \beta_4S(t)W(t)) \\ &+ \Big(1 - \frac{I_1^*}{I_1(t)}\Big)(\beta_1S(t)I_1(t) + \beta_2S(t)I_2(t) + \beta_3S(t)V(t) + \beta_4S(t)W(t) - \alpha I_1(t) \\ &- d_1I_1(t)) + \frac{\beta_2S^*c_1c_2 + c_2\beta_3S^*\delta_2 + c_1\beta_4S^*pd_2}{d_2c_1c_2}\Big(1 - \frac{I_2^*}{I_2(t)}\Big)(\alpha I_1(t) - d_2I_2(t)) \\ &+ \frac{\beta_3S^*}{c_1}\Big(1 - \frac{V^*}{V(t)}\Big)(\delta_1I_1(t) + \delta_2I_2(t) - c_1V(t)) \\ &+ \frac{\beta_4S^*}{c_2}\Big(1 - \frac{W^*}{W(t)}\Big)(pd_1I_1(t) + pd_2I_2(t) - c_2W(t)) \\ =& d_1S^*\Big(2 - \frac{S^*}{S(t)} - \frac{S(t)}{S^*}\Big) + \beta_1S^*I_1^*\Big(2 - \frac{S^*}{S(t)} - \frac{S(t)}{S^*}\Big) \\ &+ \beta_2S^*I_2^*\Big(3 - \frac{S^*}{S(t)} - \frac{I_1^*S(t)I_2(t)}{I_1(t)S^*I_2^*} - \frac{I_2^*I_1(t)}{I_2(t)I_1^*}\Big) \\ &+ \frac{\beta_3S^*\delta_1I_1^*}{c_1}\Big(3 - \frac{S^*}{S(t)} - \frac{I_1^*S(t)V(t)}{I_1(t)S^*V^*} - \frac{V^*I_1(t)}{V(t)I_1^*}\Big) \\ &+ \frac{\beta_3S^*\delta_2I_2^*}{c_2}\Big(4 - \frac{S^*}{S(t)} - \frac{I_1^*S(t)V(t)}{I_1(t)S^*V^*} - \frac{I_2^*I_1(t)}{I_2(t)I_1^*} - \frac{V^*I_2(t)}{V(t)I_2^*}\Big) \\ &+ \frac{\beta_4S^*pd_1I_1^*}{c_2}\Big(3 - \frac{S^*}{S(t)} - \frac{I_1^*S(t)W(t)}{I_1(t)S^*W^*} - \frac{W^*I_1(t)}{W(t)I_1^*}\Big) \\ &+ \frac{\beta_4S^*}{c_2}pd_2I_2^*\Big(4 - \frac{S^*}{S(t)} - \frac{I_1^*S(t)W(t)}{I_1(t)S^*W^*} - \frac{I_2^*I_1(t)}{I_2(t)I_1^*} - \frac{W^*I_2(t)}{W(t)I_2^*}\Big). \end{aligned}$$

Using $F(x) = x - 1 - \ln x, x \in (0, \infty)$, we have

$$\begin{aligned} \frac{dL_1(t)}{dt}\Big|_{(2.1)} =& -d_1S^*\Big[F\Big(\frac{S^*}{S(t)}\Big) + F\Big(\frac{S(t)}{S^*}\Big)\Big] - \beta_1S^*I_1^*\Big[F\Big(\frac{S^*}{S(t)}\Big) + F\Big(\frac{S(t)}{S^*}\Big)\Big] \\ &- \beta_2S^*I_2^*\Big[F\Big(\frac{S^*}{S(t)}\Big) + F\Big(\frac{I_1^*S(t)I_2(t)}{I_1(t)S^*I_2^*}\Big) + F\Big(\frac{I_2^*I_1(t)}{I_2(t)I_1^*}\Big)\Big] \end{aligned}$$

$$
\begin{aligned}
&- \frac{\beta_3 S^* \delta_1 I_1^*}{c_1}\Big[F\Big(\frac{S^*}{S(t)}\Big) + F\Big(\frac{I_1^* S(t) V(t)}{I_1 S^* V^*}\Big) + F\Big(\frac{V^* I_1(t)}{V(t) I_1^*}\Big)\Big] \\
&- \frac{\beta_3 S^* \delta_2 I_2^*}{c_2}\Big[F\Big(\frac{S^*}{S(t)}\Big) + F\Big(\frac{I_1^* S(t) V(t)}{I_1(t) S^* V^*}\Big) + F\Big(\frac{I_2^* I_1(t)}{I_2(t) I_1^*}\Big) + F\Big(\frac{V^* I_2(t)}{V(t) I_2^*}\Big)\Big] \\
&- \frac{\beta_4 S^* p d_1 I_1^*}{c_2}\Big[F\Big(\frac{S^*}{S(t)}\Big) + F\Big(\frac{I_1^* S(t) W(t)}{I_1(t) S^* W^*}\Big) + F\Big(\frac{W^* I_1(t)}{W(t) I_1^*}\Big)\Big] \\
&- \frac{\beta_4 S^*}{c_2} p d_2 I_2^*\Big[F\Big(\frac{S^*}{S(t)}\Big) + F\Big(\frac{I_1^* S(t) W(t)}{I_1(t) S^* W^*}\Big) + F\Big(\frac{I_2^* I_1(t)}{I_2(t) I_1^*}\Big) + F\Big(\frac{W^* I_2(t)}{W(t) I_2^*}\Big)\Big].
\end{aligned}
$$

Note that $L_1'(t) < 0$ when $R_0 > 1$. Besides, $L_1'(t) = 0$ if and only if $S(t) = S^*, I_1(t) = I_1^*, I_2(t) = I_2^*, V(t) = V^*, W(t) = W^*$. The single point set E_1 is the largest invariant set of model (2.1) on set $\{(S(t), I_1(t), I_2(t), V(t), W(t)) \in \Omega \mid L_1'(t) = 0\}$. Using LaSalle's Invariance Principle [33] and the local stability of E_1, then the endemic equilibrium E_1 is globally asymptotically stable in Ω when $R_0 > 1$. □

4. Numerical simulations

Using the public information, parameter values and initial values are estimated. This section gives the sensitivity indexes of the basic reproduction number R_0 and state variables I_1, I_2, V and W. Numerical simulations are implemented to illustrate our theoretical results and assess the impact of the virus in the environment and swill on the ASFV transmission. All simulations are conducted by Matlab.

4.1. Parameter estimation

4.1.1. Data source

In August 2018, an ASF outbreak occurred at an Aiyuan farm of Jiangsu Jiahua Breeding Pig Company in Siyang County, China. There are 14929 pigs in the 13 pigpens. The ASF outbreak is possibly caused by the introduction of contaminated vehicles and employees. The data from January 8, 2019 to January 11, 2019 are obtained from the China Animal Health Endemic Center (CAHEC) [34] and reference [35]. Our data includes new ASF cases in Table 2. All data used are from the public information.

It is worth noting that as a major pig producing country in the world, China has suffered great economic losses from the ASF outbreaks to her domestic pig market. Since there is no effective treatment for ASFV at present, the Chinese government attaches great importance to the prevention and control of ASF at an early stage. For example, when pig farmers are suspected of being infected with ASFV, the relevant departments will immediately conduct an epidemiological investigation and clinical diagnosis, and collect samples for testing in a short time. Once the outbreak of the epidemic is determined, all pigs in the epidemic site and within a certain range should be culled immediately [10]. At the same time, carcasses and pollutants should be destroyed innocuously, and vehicles, facilities and relevant personnel in the epidemic site should be disinfected and cleaned. Further intervention measures will be implemented according to the development of the epidemic, including restrictions on the movement of pigs and pork products, timely monitoring and quarantine. Therefore, the epidemic foci usually only have time series data within a few days.

Table 2. Daily new infectious pigs in Aiyuan.

Date	No. of infectious pigs
Jan. 8, 2019	48
Jan. 9, 2019	87
Jan. 10, 2019	102
Jan. 11, 2019	196

4.1.2. Parameter estimation

Based on our mathematical model and the cumulative number of ASF cases and using the Least Square method (LSM), our model is fitted to the real data. Parameters values β_3 and α and initial values $I_1(0)$ with 95% confidence interval (CI) are estimated in Tables 3 and 4. Other parameter values are obtained from the real data and references.

4.1.3. Fitting results

Given the uncertainty of parameter values and initial values, LSM is used to assess our model with evaluated parameter values and initial values in Tables 3 and 4. Figure 10 gives the estimated cumulative number of ASF cases with real data on the Aiyuan pig farm. Our simulations are consistent with the real data, which verifies the accuracy of the model.

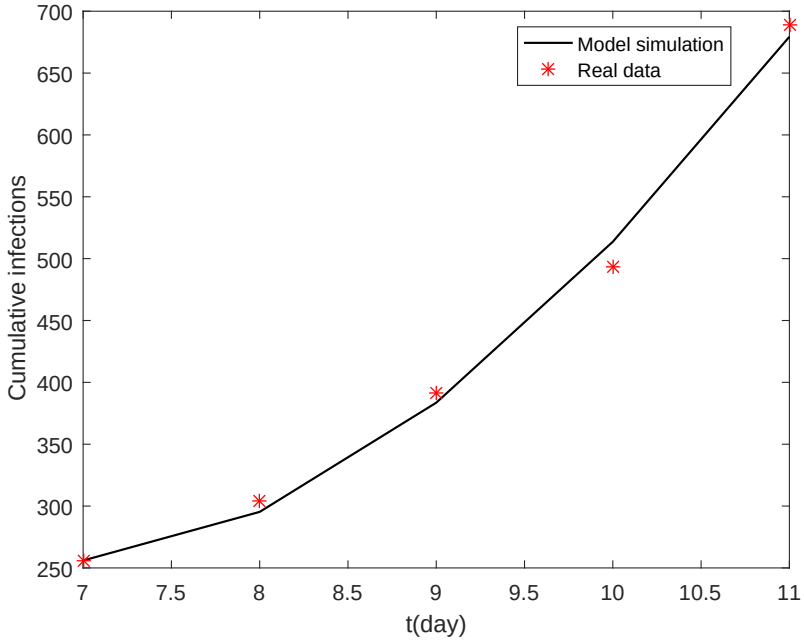

Figure 2. The fitting results of estimated cumulative number of ASF cases with real data.

Table 3. Related parameters in model (2.1).

Parameter	Description	Value (Range)	95% CI	Source
b	The recruitment rate of pigs	$[9\times10^3, 1.1\times10^4]$	-	[28]
β_1	The transmission rate from asymptomatic infectious pigs to susceptible pigs	$[9\times10^{-7}, 1.1\times10^{-8}]$	-	[36]
β_2	The transmission rate from symptomatic infectious pigs to susceptible pigs	$[1.35\times10^{-8}, 1.65\times10^{-7}]$	-	[37]
β_3	The transmission rate from virus in environment to susceptible pigs	1.28×10^{-9}	$[1.49\times10^{-10}, 1.49\times10^{-9}]$	Fitted
β_4	The transmission rate from swill to susceptible pigs	$[2.7\times10^{-10},\ 3.3\times10^{-10}]$	-	[28]
d_1	The removal rate of asymptomatic infectious pigs including slaughtering and death	[0.002, 0.0035]	-	[26]
d_2	The removal rate of symptomatic infectious pigs including slaughtering and death	[0.4, 0.6]	-	[37]
c_1	The clearance rate of virus in environment	[0.05, 0.1]	-	[35]
c_2	The clearance rate of swill	[0.011, 0.0035]	-	[28]
δ_1	The release rate of ASFV from asymptomatic infectious pigs	[1, 9]	-	[35]
δ_2	The release rate of ASFV from symptomatic infectious pigs	[1, 9]	-	[28]
p	The proportion of pig products from infectious pigs to swill	[0.1, 1]	-	[28]
α	The transfer rate from asymptomatic infectious pigs to symptomatic infectious pigs	0.157	[0.12, 0.35]	Fitted

Table 4. The initial values in Aiyuan.

Initial values	Description	Value	95%CI	Source
$I_1(0)$	Initial value of asymptomatic pigs	256	[254, 256]	Fitted
$S(0)$	Initial value of susceptible pigs	14929	-	Data
$I_2(0)$	Initial value of symptomatic pigs	0	-	Data
$V(0)$	Initial value of virus load in the environment	2.6×10^7	-	Data
$W(0)$	Initial value of contaminated swills	0	-	Data

4.2. Sensitivity analysis

Partial rank correlation coefficients (PRCCs) and variance decomposition (obtained by an extended version of the Fourier Amplitude Sensitivity Test (eFAST)) are used to carry out the sensitivity analysis [38]. We calculate PRCCs and eFAST sensitivity indexes of R_0 and I_1, I_2, V, W to have a complete and informative uncertainty and sensitivity (US) analysis.

4.2.1. Sensitivity indexes of R_0

The PRCCs and eFAST sensitivity results about R_0 are illustrated in Figure 3 using the bar charts. PRCCs in Figure 3 give that b, β_2, δ_1, d_1, c_1, α and δ_2 have a significant impact on R_0. The first order S_i and the total order S_{Ti} are given for each parameter (including a dummy parameter) in Figure 3. The red bar represents the sum of the influence of a single parameter and its interaction with other parameters, denoted as S_{Ti} (total order sensitivity index) and the blue bar indicates the sensitivity of the independent effect of a single parameter, expressed as S_i (first-order sensitivity index). Considering only $p < 0.01$, the relationship of S_i is $c_1 > \delta_1 > \alpha > d_1 > b > \beta_2$, and the size relationship of S_{Ti} is $\delta_1 > \alpha > c_1 > d_1 > b > \beta_2$.

Therefore, Figure 3 finds that b, β_2, δ_1 and δ_2 have a significant positive impact on R_0, while d_1, c_1 and α have a significant negative impact on R_0. However, b and β_2 have high PRCCs sensitivity indexes and low eFAST sensitivity indexes.

4.2.2. Sensitivity indexes of I_1, I_2, V, W

To evaluate whether the importance of a parameter appears in the entire time interval during the dynamics process, we focus on state variables I_1, I_2, V and W. We assume that the PRCCs and eFAST time ranges from 0 to 30, and parameter values are chosen from Table 1. We calculate the PRCCs and eFAST (S_i) indexes at multiple time points and plot the time series about state variables I_1, I_2, V and W. The gray area indicates that there is no significant difference from zero.

In Figure 4(a), the parameters are divided into four categories. The PRCCs index values of the first category including $\delta_1, \delta_2, \beta_3, b$ and c_1 firstly rise or fall to a value over time, and then gradually stabilize. The PRCCs index values of the second category including β_2 rise to a peak at an average speed, and then decrease rapidly until there is no significant difference from zero. The PRCCs index values of the third category including α always remain in a steady correlation with I_1. The fourth category containing $\beta_4, d_2, c_2, d_1, \beta_1$ and p have no effect on I_1. Figure 4(b) reveals that the curve of

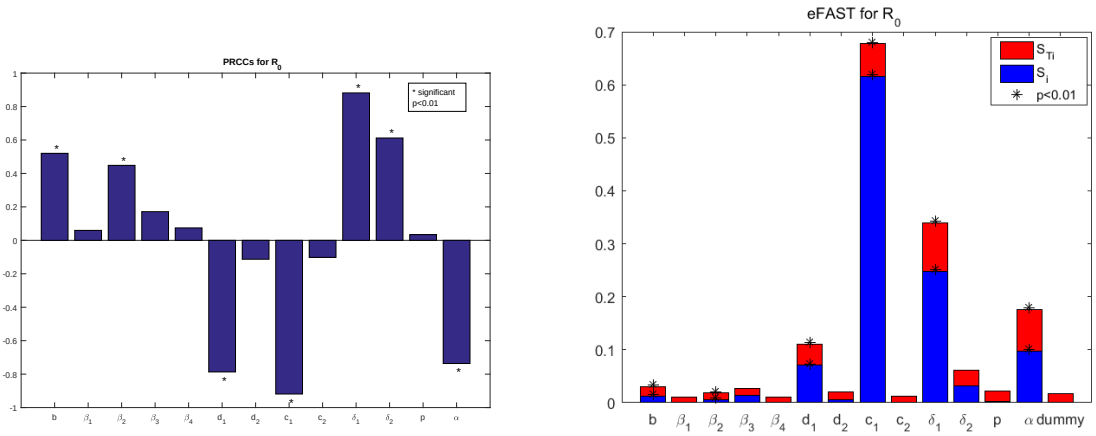

(a) (b)

Figure 3. (a) PRCCs sensitivity indexes of R_0; (b) eFAST sensitivity indexes of R_0.

the parameter α is very stable at early time points, and declines after 15 days and then stabilize in the future.

Figure 5(a) shows that the curve of parameter α is positively correlated with I_2 at the initial stage, and then decreases rapidly to negative correlation until gradually reaches a stable state. Figure 5(b) shows that α and d_2 have a significant impact on I_2.

Figure 6(a) demonstrates that δ_1 and δ_2 have a strong positive impact on V and c_1 is negatively correlated with V. Figure 6(b) demonstrates that δ_1 has a strong positive impact on V.

Figure 7(a) explains that α and p have a strong positive impact on W and c_2 is negatively correlated with W. Figure 7(b) explains that p has a strong positive impact on W.

4.3. Numerical simulations

In this section, numerical simulations are implemented to illustrate our theoretical results and assess the impact of the virus in the environment and swill on the ASFV transmission.

Set parameters $b = 10587$, $\beta_1 = 1.0004 \times 10^{-8}$, $\beta_2 = 5.5410 \times 10^{-8}$, $\beta_3 = 3.0947 \times 10^{-10}$, $\beta_4 = 3.2320 \times 10^{-10}$, $c_1 = 0.0391, c_2 = 0.0545$, $d_1 = 0.0035$, $d_2 = 0.5885$, $\delta_1 = 1.5977$, $\delta_2 = 2.4596$, $p = 0.1285$, $\alpha = 0.1555$, and the initial values $S(0) = 10000$, $I_1(0) = 256$, $I_2(0) = 0$, $V(0) = 1000$, $W(0) = 300$. We get that the basic reproduction number $R_0 = 0.8015 < 1$, and the disease-free equilibrium of model (2.1) is globally asymptotically stable (Figure 8(a)), which illustrates the results in Theorem 3.3.

Set parameters $b = 10358$, $\beta_1 = 1.0272 \times 10^{-8}$, $\beta_2 = 1.5669 \times 10^{-7}$, $\beta_3 = 4.2918 \times 10^{-10}$, $\beta_4 = 3.1256 \times 10^{-10}$, $c_1 = 0.0377, c_2 = 0.0725$, $d_1 = 0.0024$, $d_2 = 0.4239$, $\delta_1 = 4.6698$, $\delta_2 = 6.2956$, $p = 0.7933$, $\alpha = 0.1439$, and the initial values $S(0) = 10000$, $I_1(0) = 256$, $I_2(0) = 0$, $V(0) = 1000$, $W(0) = 300$. We obtain that the basic reproduction number $R_0 = 4.1865 > 1$, and the unique endemic equilibrium is globally asymptotically stable (Figure 8(b)), which illustrates the results in Theorem 3.4.

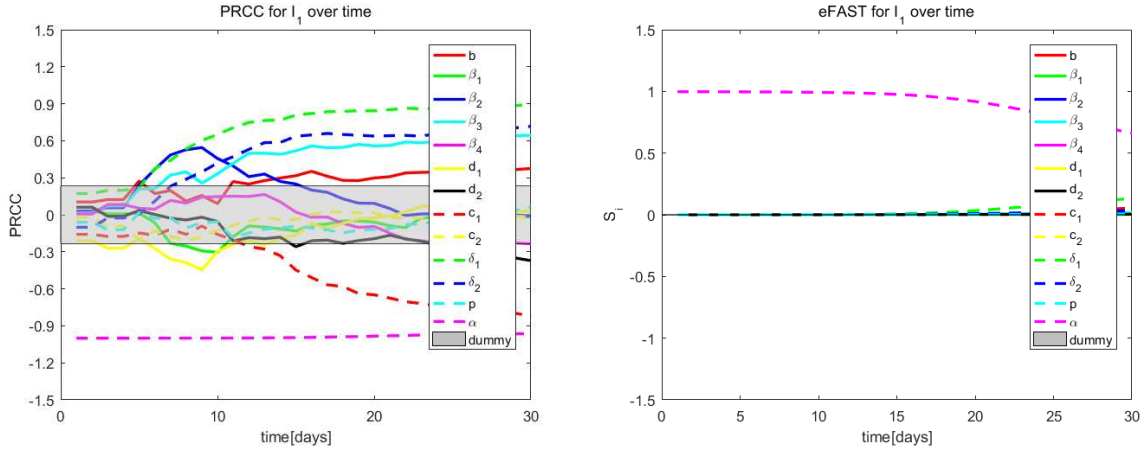

(a) (b)

Figure 4. (a) Time-varying PRCCs sensitivity indexes of I_1; (b) Time-varying first-order sensitivity indexes S_i of I_1.

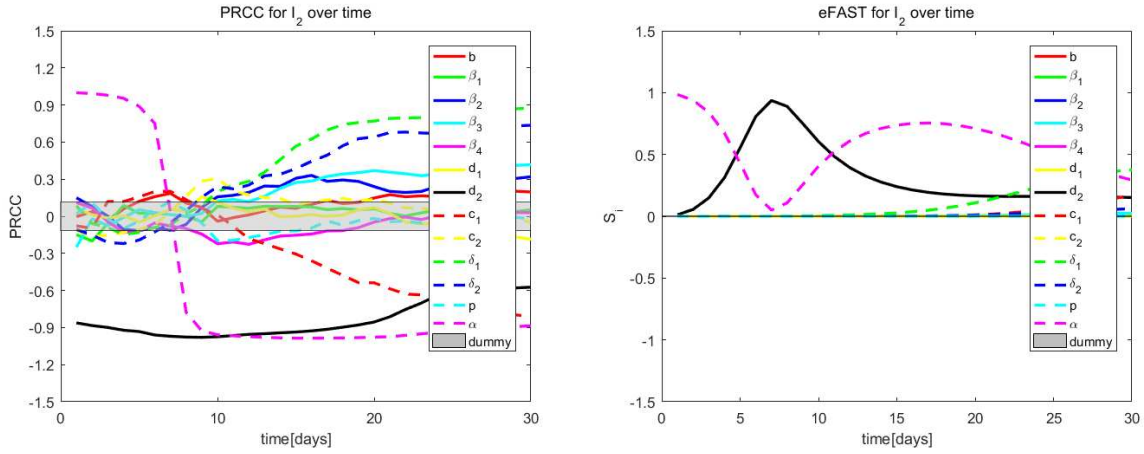

(a) (b)

Figure 5. (a) Time-varying PRCC sensitivity indexes of I_2; (b) Time-varying first-order sensitivity indexes S_i of I_2.

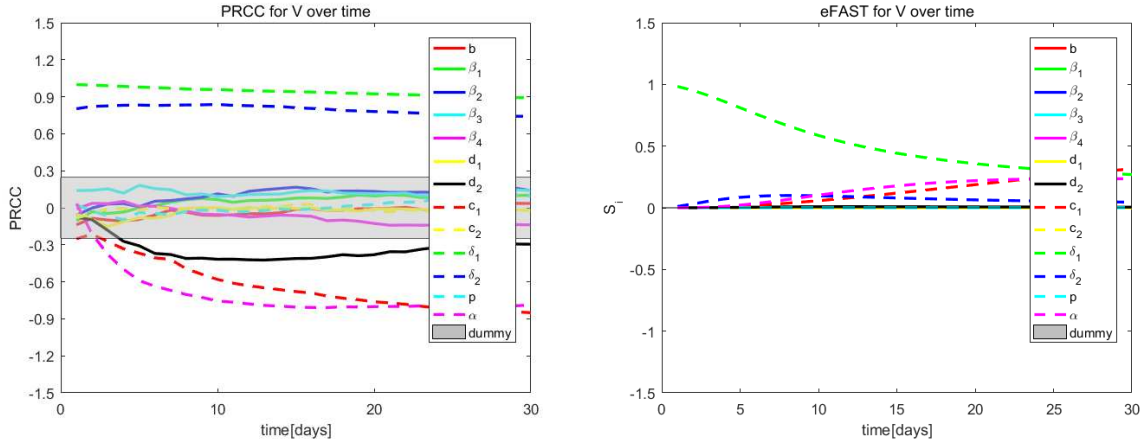

(a) (b)

Figure 6. (a) Time-varying PRCC sensitivity indexes of V; (b) Time-varying first-order sensitivity indexes S_i of V.

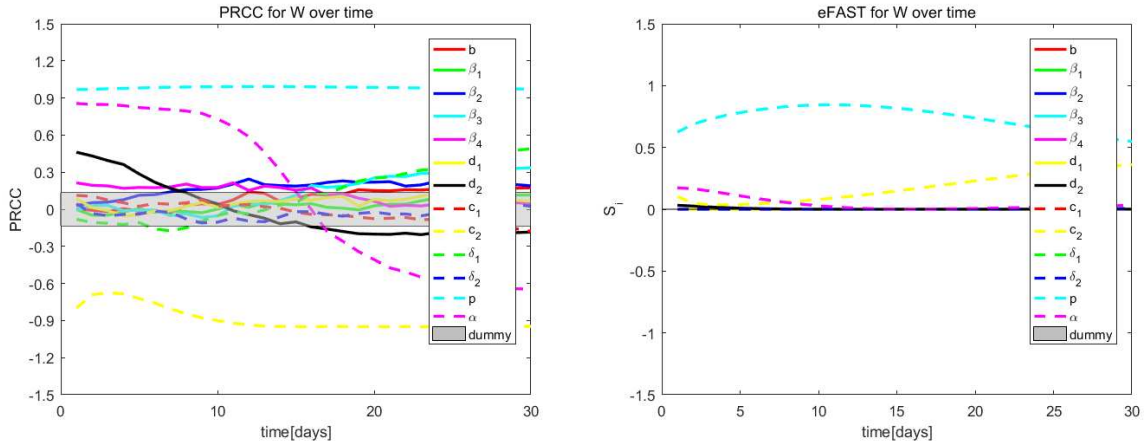

(a) (b)

Figure 7. (a) Time-varying PRCC sensitivity indexes of W; (b) Time-varying first-order sensitivity indexes S_i of W.

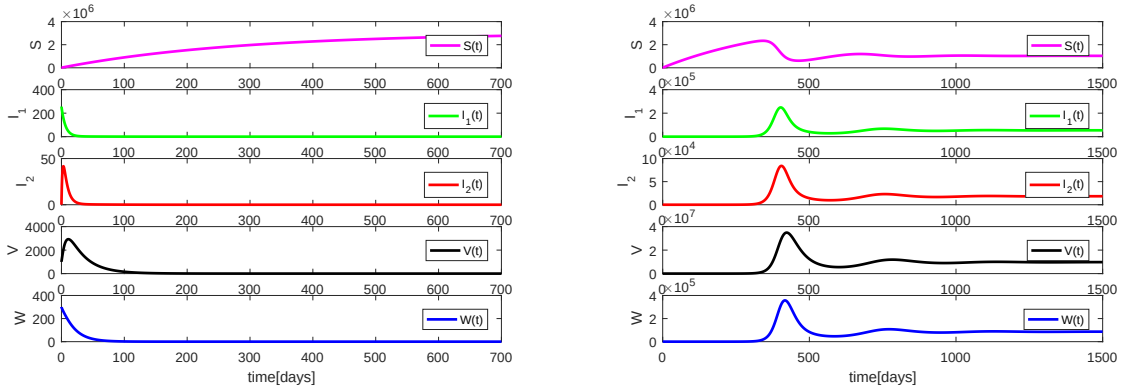

(a) (b)

Figure 8. (a) When $R_0 < 1$, the disease-free equilibrium E_0 is globally asymptotically stable. (b) When $R_0 > 1$, the endemic equilibrium E_1 is globally asymptotically stable.

4.3.1. The effect of the virus in the environment on the ASFV transmission

The effect of the virus in the environment on the ASFV transmission is assessed by the impact of δ_1 and δ_2 on the symptomatic ASF cases. Set $\delta_1 = 9$, $\delta_1 = 6$ and $\delta_1 = 3$, the peak value and peak time of symptomatic ASF cases could reach 780, 660, 570 and 60, 63, 65 days, respectively. If $\delta_2 = 9$, $\delta_2 = 6$ and $\delta_2 = 3$, the peak value of symptomatic ASF cases could reach 630, 590 and 550, respectively, and the peak time of symptomatic ASF cases could roughly the same. Figure 9 reveals that virus in the environment increases the peak value of symptomatic ASF cases.

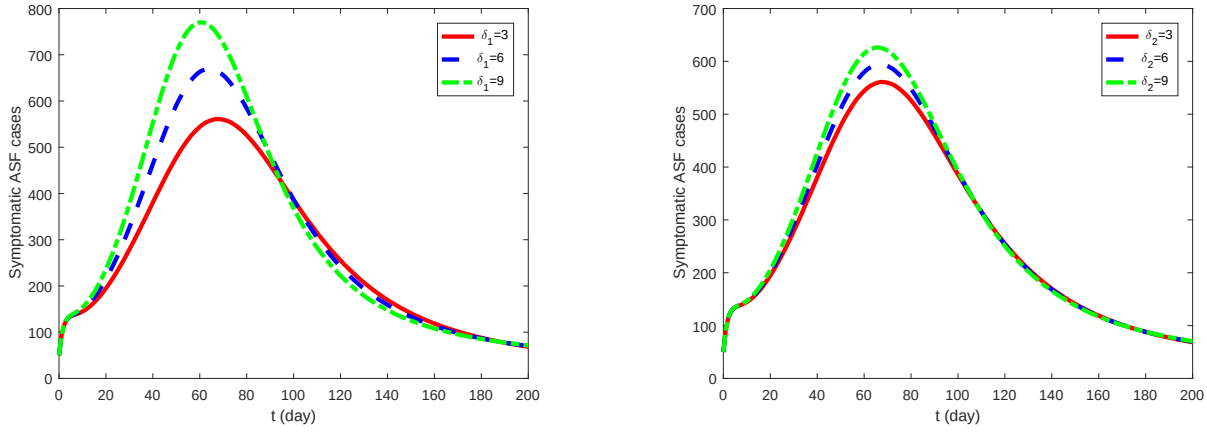

(a) (b)

Figure 9. The effect of virus in environment on the symptomatic ASF cases.

4.3.2. The effect of swill on the ASFV transmission

The effect of swill on the ASFV transmission is assessed by the impact of p on the symptomatic ASF cases. If $p = 0.8$, $p = 0.6$ and $p = 0.5$, the peak value of symptomatic ASF cases could reach

820, 650, 550 and 59, 65, 70 days, respectively. Figure 10 reveals that contaminated swill increases the peak value of symptomatic ASF cases and makes the peak time in advance.

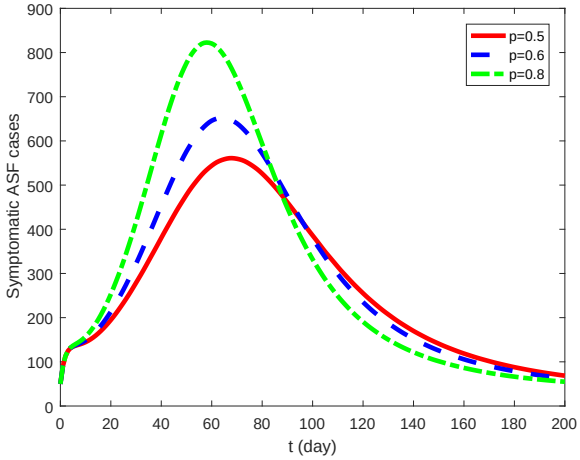

Figure 10. The effect of swill on the symptomatic ASF cases.

5. Conclusions

African swine fever is listed as an animal disease that must be reported by the World Organization of Animal Health (OIE), and is a class I animal disease in China. The early epidemic in China mainly occurred in small and medium-sized pig farms, which was mainly caused by swill feeding [28]. Due to the 100% mortality rate, ASF seriously threatens the pig industry. The virus in the environment and contaminated swill contribute to the ASFV transmission. To study the impact of the virus in the environment and contaminated swill on the ASFV transmission, we build the ASFV transmission model with the virus in the environment and swill.

This is the first study to show the global dynamics of the ASFV transmission model. We compute the basic reproduction number, and prove the global stability of disease-free equilibrium and endemic equilibrium. When $R_0 < 1$, the disease-free equilibrium E_0 is globally asymptotically stable. When $R_0 > 1$, the unique endemic equilibrium E_1 is globally asymptotically stable.

Our findings reveal that the release rate of ASFV from asymptomatic and symptomatic infectious pigs and the proportion of pig products from infectious pigs to swill have a significant impact on the ASFV transmission. We use the PRCCs and eFAST to evaluate the impact of parameters on R_0 and I_1, I_2, V, W. PRCCs and eFAST sensitivity analysis reveals that parameters b, β_2 and δ_1 have a significant positive effect on R_0, and parameters d_1, c_1 and α have a significant negative effect on R_0. The sensitivity indexes at multiple time points give that the release rate of ASFV from asymptomatic and symptomatic infectious pigs and the proportion of pig products from infectious pigs to swill have a significant impact on I_1, I_2, V and W.

The results show that viruses in the environment and contaminated swill contribute to the ASFV transmission. PRCCs and eAFST indicate that δ_1 and c_1 have a significant effect on R_0, which means that the virus in the environment exerts a major influence on R_0. PRCCs and eAFST indicate that δ_1, δ_2 and p have a significant impact on I_1, I_2, V and W, which means that the virus in the environment

and contaminated swill exert a major influence on I_1, I_2, V and W. Numerical simulations reveal that reducing δ_1 and δ_2 could effectively cut down the peak value of symptomatic ASF cases, and increasing p could reduce the peak value of symptomatic ASF cases by over 30%.

Our results indicate that contaminated swill contributes to the ASFV transmission, which is consistent with the results in [28]. Therefore, banning swill feeding, improving farmers' awareness of swill transmission and large-scale breeding are very necessary for prevention and control measures, which can effectively reduce the risk of ASFV transmission. Furthermore, our results show that the virus in the environment greatly accelerates ASFV transmission. By increasing the frequency and efficiency of disinfection, removing dead pigs in time, and strictly testing the vehicles and staff entering and leaving the pig farm, the virus in the environment could be cleared to control the epidemic.

It is of great significance to study the impact of culling on ASFV transmission. Millions of pigs are culled to contain the ASFV transmission in China. For future work, we may evaluate the impact of culling on the ASFV transmission. In this paper, our findings may help animal health to prevent and control the ASFV transmission.

Acknowledgments

The research is supported by the National Natural Science Foundation of China (12171291, 11871179, 61873154), the Fund Program for the Scientific Activities of Selected Returned Overseas Professionals in Shanxi Province (20200001), the Fundamental Research Program of Shanxi Province (20210302124018), the Shanxi Scholarship Council of China (HGKY2019004), and the Scientific and Technological Innovation Programs (STIP) of Higher Education Institutions in Shanxi (2019L0082).

Conflict of interest

The authors declare there is no conflict of interest.

Availability of data and materials

The ASF reported data used in this work were freely obtained from the China Animal Health Endemic Center via https://www.cahec.cn/ and reference [35].

References

1. C. Alonso, M. Borca, L. Dixon, Y Revilla, F. ROdriguez, J. M. Escribano, ICTV virus taxonomy profile: Asfarviridae, *J. Gen. Virol.*, **99** (2018), 613–614. https://doi.org/10.1099/jgv.0.001049
2. C. M. Fauquet, M. A. Mayo, J. Maniloff, U. Desselberger, L. A. Ball, *Virus taxonomy: VIIIth report of the International Committee on Taxonomy of Viruses*, Academic Press, 2005.
3. S. Costard, B. Wieland, W. De Glanville, F. Jori, R. Rowlands, W. Vosloo, et al., African swine fever: how can global spread be prevented?, *Phil. Trans. R. Soc. B*, **364** (2009), 2683–2696. https://doi.org/10.1098/rstb.2009.0098
4. C. Guinat, A. Gogin, S. Blome, G. Keil, R. Pollin, D. U. Pfeiffer, et al., Transmission routes of

African swine fever virus to domestic pigs: current knowledge and future research directions, *Vet. Rec.*, **178** (2016), 262–267. https://doi.org/10.1136/vr.103593

5. H. Nishiura, Early efforts in modeling the incubation period of infectious diseases with an acute course of illness, *Emerg. Themes Epidemiology*, **4** (2007), 1–12. https://doi.org/10.1186/1742-7622-4-2
6. I. Galindo, C. Alonso, African swine fever virus: a review, *Viruses*, **9** (2017), 103. https://doi.org/10.3390/v9050103
7. C. J. Quembo, F. Jori, W. Vosloo, L. Health, Genetic characterization of African swine fever virus isolates from soft ticks at the wildlife/domestic interface in Mozambique and identification of a novel genotype, *Transbound. Emerg. Dis.*, **65** (2018), 420–431. https://doi.org/10.1111/tbed.12700
8. E. R. Tulman, G. A. Delhon, B. K. Ku, D. L. Rock, *African Swine Fever Virus. In: Van Etten, J.L. (eds) Lesser Known Large dsDNA Viruses. Current Topics in Microbiology and Immunology*, *Springer*, Berlin, Heidelberg, 2009. https://doi.org/10.1007/978-3-540-68618-7_2
9. X. Shen, Z. Pu, Y. Li, S. Yu, F. Guo, T. Luo, et al., Phylogeographic patterns of the African swine fever virus, *J. Infect.*, **79** (2019), 174–187. https://doi.org/10.1016/j.jinf.2019.05.004
10. T. Wang, Y. Sun, H. J. Qiu, African swine fever: an unprecedented disaster and challenge to China, *Infec. Dis. Poverty*, **7** (2018), 66–70. https://doi.org/10.1186/s40249-018-0495-3
11. J. Bao, Q. Wang, P. Lin, C. Liu, L. Li, X. Wu, et al., Genome comparison of African swine fever virus China/2018/AnhuiXCGQ strain and related European p72 Genotype II strains, *Transbound. Emerg. Dis.*, **66** (2019), 1167–1176. https://doi.org/10.1111/tbed.13124
12. X. Zhou, N. Li, Y. Luo, Y. E. Liu, F. Miao, T. Chen, et al., Emergence of African swine fever in China, 2018, *Transbound. Emerg. Dis.*, **65** (2018), 1482–1484. https://doi.org/10.1111/tbed.12989
13. S. Ge, J. Li, X. Fan, F. Liu, L. Li, Q. Wang, et al., Molecular characterization of African swine fever virus, China, 2018, *Emerg. Infect. Dis.*, **24** (2018), 2131–2133. https://doi.org/10.3201/eid2411.181274
14. Q. Wang, W. Ren, J. Bao, S. Ge, J. Li, L. Li, et al., The first outbreak of African swine fever was confirmed in China, *China Animal Health Inspection*, **35** (2018), 1–4. https://doi.org/10.3969/j.issn.1005-944X.2018.09.001
15. Y. Wang, L. Gao, Y. Li, Q. Xu, H. Yang, C. Shen, et al., African swine fever in China: Emergence and control, *J. Biosaf. Biosecur.*, **1** (2019), 7–8. https://doi.org/10.1016/j.jobb.2019.01.006
16. H. Song, W. Jiang, S. Liu, Global dynamics of two heterogeneous SIR models with nonlinear incidence and delays, *Int. J. Biomath.*, **9** (2016), 1650046. https://doi.org/10.1142/S1793524516500467
17. H. Song, S. Liu, W. Jiang, Global dynamics of a multistage SIR model with distributed delays and nonlinear incidence rate, *Math. Methods Appl. Sci.*, **40** (2017), 2153–2164. https://doi.org/10.1002/mma.4130
18. H. Song, F. Li, Z. Jia, Z. Jin, S. Liu, Using traveller-derived cases in Henan Province to quantify the spread of COVID-19 in Wuhan, China, *Nonlinear Dyn.*, **101** (2020), 1821–1831. https://doi.org/10.1007/s11071-020-05859-1

19. H. Song, Z. Jia, Z. Jin, S. Liu, Estimation of COVID-19 outbreak size in Harbin, China, *Nonlinear Dyn.*, **106** (2021), 1229–1237. https://doi.org/10.1007/s11071-021-06406-2
20. H. Song, G. Fan, S. Zhao, H. Li, Q. Huang, D. He, Forecast of the COVID-19 trend in India: a simple modelling approach, *Math. Biosci. Eng.*, **18** (2021), 9775–9786. https://doi.org/10.3934/mbe.2021479
21. H. Song, G. Fan, Y. Liu, X. Wang, D. He, The Second Wave of COVID-19 in South and Southeast Asia and the Effects of Vaccination, *Front. Med.*, **8** (2021), 773110. https://doi.org/10.3389/fmed.2021.773110
22. H. Song, F. Liu, F. Li, C. Cao, H. Wang, Z. Jia, et al., Modeling the second outbreak of COVID-19 with isolation and contact tracing, *Discrete Cont. Dyn.-B*, **27** (2022), 5757–5777. https://doi.org/10.3934/dcdsb.2021294
23. H. Song, Z. Jin, C. Shan, L. Chang, The spatial and temporal effects of Fog-Haze pollution on the influenza transmission, *Int. J. Biomath.*, (2022), 2250096. https://doi.org/10.1142/S1793524522500966
24. F. I. Korennoy, V. M. Gulenkin, A. E. Gogin, T. Vergne, A. K. Karaulov, Estimating the basic reproductive number for African swine fever using the Ukrainian historical epidemic of 1977, *Transbound. Emerg. Dis.*, **64** (2017), 1858–1866. https://doi.org/10.1111/tbed.12583
25. C. Guinat, A. L. Reis, C. L. Netherton, L. Goatley, D. U. Pfeiffer, L.Dixon, Dynamics of African swine fever virus shedding and excretion in domestic pigs infected by intramuscular inoculation and contact transmission, *Vet. Res.*, **45** (2014), 1–9. https://doi.org/10.1186/s13567-014-0093-8
26. M. B. Barongo, R. P. Bishop, E. M. Fevre, D. L. Knobel, A. Ssematimba, A mathematical model that simulates control options for African swine fever virus (ASFV), *PLoS One*, **11** (2016), e0158658. https://doi.org/10.1371/journal.pone.0158658
27. X. O'Neill, A. White, F. Ruiz-Fons, C. Gortazar, Modelling the transmission and persistence of African swine fever in wild boar in contrasting European scenarios, *Sci. Rep.*, **10** (2020), 1–10. https://doi.org/10.1038/s41598-020-62736-y
28. J. Li, Z. Jin, Y. Wang, X. Sun, Q. Xu, J. Kang, et al., Data-driven dynamical modelling of the transmission of African swine fever in a few places in China, *Transbound. Emerg. Dis.*, **69** (2021), e646–e658. https://doi.org/10.1111/tbed.14345.
29. J. M. Sanchez-Vizcaino, L. Mur, J. C. Gomez-Villamandos, L. Carrasco, An update on the epidemiology and pathology of African swine fever, *J. Comp. Pathol.*, **152** (2015), 9–21. https://doi.org/10.1016/j.jcpa.2014.09.003
30. M. Arias, J. M. Sanchez-Vizcaino, A. Morilla, K. J. Yoon, J. J. Zimmerman, African swine fever, *Trends in emerging viral infections of swine*, (2002), 119–124.
31. H. K. Khalil, *Nonlinear Systems*, New York: *Macmillan Co.*, 1992.
32. P. van den Driessche, J. Watmough, Reproduction numbers and sub-threshold endemic equilibria for compartmental models of disease transmission, *Math. Biosci.*, **180** (2002), 29–48. https://doi.org/10.1016/S0025-5564(02)00108-6
33. Lasalle J. *The Stability of Dynamical Systems*, SIAM, Philadelphia, 1976.
34. The China Animal Health Endemic Center, https://www.cahec.cn/.

35. X. Zhang, X. Rong, J. Li, M. Fan, Y. Wang, X. Sun, et al., Modeling the outbreak and control of African swine fever virus in large-scale pig farms, *J. Theor. Biol.*, **526** (2021), 110798. https://doi.org/10.1016/j.jtbi.2021.110798

36. M. B. Barongo, K. Stahl, B. Bett, R. P. Bishop. E. M. Fevre, T. Aliro, et al., Estimating the basic reproductive number (R_0) for African swine fever virus (ASFV) transmission between pig herds in Uganda, *PloS One*, **10** (2015), e0125842. https://doi.org/10.1371/journal.pone.0125842

37. M. B. Bitamale, *Modelling the transmission dynamics and the effect of different control strategies for African swine fever virus in East Africa*, Ph.D thesis, University of Pretoria, 2018. http://hdl.handle.net/2263/67858

38. S. Marino, I. B. Hogue, C. J. Ray, D. E. Kirschner, A methodology for performing global uncertainty and sensitivity analysis in systems biology, *J. Theor. Biol.*, **254** (2008), 178–196. https://doi.org/10.1016/j.jtbi.2008.04.011

AIMS Press